NMR docking of the competitive inhibitor thymidine 3′,5′-diphosphate into the X-ray structure of Staphylococcal nuclease

ARTICLE *in* PROTEINS STRUCTURE FUNCTION AND BIOINFORMATICS · SEPTEMBER 1993

Impact Factor: 2.63 · DOI: 10.1002/prot.340170106 · Source: PubMed

5 AUTHORS, INCLUDING:

David Joseph Weber
University of Maryland, Baltimore
126 PUBLICATIONS **3,837** CITATIONS
SEE PROFILE

Engin H. Serpersu
University of Tennessee
86 PUBLICATIONS **1,734** CITATIONS
SEE PROFILE

Apostolos G Gittis
National Institute of Allergy and Infectious …
42 PUBLICATIONS **2,103** CITATIONS
SEE PROFILE

Eaton E Lattman
University at Buffalo, The State University o…
123 PUBLICATIONS **4,099** CITATIONS
SEE PROFILE

PROTEINS: Structure, Function, and Genetics 17:20–35 (1993)

NMR Docking of the Competitive Inhibitor Thymidine 3′,5′-Diphosphate Into the X-Ray Structure of Staphylococcal Nuclease

David J. Weber,[1] Engin H. Serpersu,[2] Apostolos G. Gittis,[2] Eaton E. Lattman,[2] and Albert S. Mildvan[1]

Departments of [1]Biological Chemistry and [2]Biophysics and Biophysical Chemistry, The Johns Hopkins University School of Medicine, Baltimore, Maryland 21205

ABSTRACT **In the X-ray structure of the ternary staphylococcal nuclease–Ca^{2+}–3′,5′-pdTp complex, the conformation of the bound inhibitor 3′,5′-pdTp is distorted by Lys-70* and Lys-71* from an adjacent molecule of the enzyme in the crystal lattice (Loll, P. J. and Lattman, E. E. Proteins 5:183–201, 1989; Serpersu, E. H., Hibler, D. W., Gerlt, J. A., and Mildvan, A. S. Biochemistry 28:1539–1548, 1989). Since this interaction does not occur in solution, the NMR docking procedure has been used to correct this problem. Based on 8 Co^{2+}–nucleus distances measured by paramagnetic effects on T_1, and 9 measured and 45 lower limit interproton distances determined by 1D and 2D NOE studies of the ternary Ca^{2+} complex, the conformation of enzyme-bound 3′,5′-pdTp is high-anti (χ = 58 ± 10°) with a C2′ endo/O1′ endo sugar pucker (δ = 143 ± 2°), (−) synclinal about the C3′–O3′ bond (ϵ = 273 ± 4°), trans, gauche about the C4′–C5′ bond (γ = 301 ± 29°) and either (−) or (+) clinal about the C5′–O5′ bond (β = 92 ± 8° or 274 ± 3°). The structure of 3′,5′-pdTp in the crystalline complex differs due to rotations about the C4′–C5′ bond (γ = 186 ± 12°, gauche, trans) and the C5′–O5′ bond [β = 136 ± 10°, (+) anticlinal]. The undistorted conformation of enzyme-bound metal–3′,5′-pdTp determined by NMR was docked into the X-ray structure of the enzyme, using 19 intermolecular NOEs from ring proton resonances of Tyr-85, Tyr-113, and Tyr-115 to proton resonances of the inhibitor. van der Waals overlaps were then removed by energy minimization. Subsequent molecular dynamics and energy minimization produced no significant changes, indicating the structure to be in a global rather than in a local minimum. While the metal-coordinated 5′-phosphate of the NMR-docked structure of 3′,5′-pdTp overlaps with that in the X-ray structure, and similarly receives bifunctional hydrogen bonds from both Arg-35 and Arg-87, the thymine, deoxyribose, and 3′-phosphate are significantly displaced from their positions in the X-ray structure, with the 3′-phosphate receiving hydrogen bonds from Lys-49 rather than from Lys-84 and Tyr-85. The repositioned thymine ring permits hydrogen bonding to the phenolic hydroxyl of Tyr-115. These new interactions, found in the NMR docked structure, are supported by reduced affinities for 3′,5′-pdTp by appropriate mutants of staphylococcal nuclease (Chuang, W.-J., Weber, D.J., Gittis, A.G., and Mildvan, A.S. (1993) accompanying paper, this issue). An inner sphere, rather than a second sphere water ligand of the metal, is optimally positioned to donate a hydrogen bond to Glu-43 and to attack the coordinated 5′-phosphate with inversion. It is concluded that the NMR docking procedure can be used to correct structural artifacts created by lattice contacts in crystals, when they occur at or near ligand binding sites, such as the active sites of enzymes.**

Key words: staphylococcal nuclease active site, conformation of 3′,5′-pdTp, lattice contacts, metal-nucleus distances, nuclear Overhauser effect

INTRODUCTION

Staphylococcal nuclease is a Ca^{2+}-activated endonuclease and exonuclease which catalyzes the hydrolysis of phosphodiester linkages in both DNA and RNA to yield 3′-nucleotides.[1,2] The substrate binding site has been proposed as consisting of three sub-

*Abbreviations used: 3′,5′-pdTp, thymidine 3′,5′-diphosphate; Tris-HCl, tris-(hydroxymethyl)aminomethane hydrochloride; NOE, nuclear Overhauser effect; EDTA, ethylene-diaminetetraacetic acid; TES, *N*-[tris(hydroxymethyl)-methyl]-2-aminoethane sulfonic acid; Lys-70*, 71*, lysine residues from a neighboring molecule of staphylococcal nuclease in the crystal lattice.

Received February 8, 1993; revision accepted April 19, 1993.

Address reprint requests to Dr. Albert S. Mildvan, Department of Biological Chemistry, The Johns Hopkins University School of Medicine, 725 North Wolfe Street, Baltimore, MD 21205-2185.

Engin H. Serpersu's current address is the Department of Biochemistry, University of Tennessee, Knoxville, TN 37996.

sites, one for each residue of a trinucleotide substrate, based on the effects of the chain length of oligonucleotide inhibitors on their K_i values.[3] In agreement with this proposal, three subsites for nucleotides have been located in the X-ray structure of staphylococcal nuclease by NMR docking of the dinucleotide dTdA and its enlargement to a trinucleotide by model building.[4,5] While the ground state structure of the enzyme metal–substrate complex is thus available, a transition state structure would be desirable in order to better comprehend the mechanism. At present, the best approximation of a transition state structure is that of the ternary enzyme–metal–3′,5′-pdTp* product complex. The potent inhibitor 3′,5′-pdTp binds to the enzyme–Ca^{2+} complex 1400-fold more tightly than does the substrate dTdA[4] and, like a phosphorane transition state, has an extra negative charge on the 5′-phosphate.

Unfortunately, the structure of enzyme-bound 3′,5′-pdTp in the crystalline state is distorted by Lys-70* and 71* from a neighboring molecule in the crystal lattice. Lys-70* inserts itself between the 5′- and 3′-phosphates spreading them apart, and Lys-71* interacts with Glu-43 the general base.[6,7] The earliest evidence for distortion of the enzyme-bound 3′,5′-pdTp by this lattice artifact was provided by differing metal–phosphorus distances found in the crystalline and dissolved ternary enzyme–metal–3′,5′-pdTp complexes. Thus in the crystal, Ca^{2+} was 3.94 ± 0.2 Å from the 5′-P and 9.82 ± 0.2 Å from the 3′-P[7] while in the ternary complex in solution, the corresponding Co^{2+}–phosphorus distances were 2.7 ± 0.5 and 4.4 ± 0.9 Å, respectively.[6] Independent evidence for a differing environment for the 3′-phosphate (but not for the 5′-phosphate) of 3′,5′-pdTp in the ternary complex in the crystal versus that in solution was a change in the chemical shift of the upfield (3′-P) resonance but not of the downfield (5′-P) resonance on crystallizing the complex as detected by comparative solution and solid state ^{31}P NMR.†

To eliminate this crystallographic artifact, attempts have been made to grow crystals of the ternary complex of the mutant K70S/K71S, but these attempts have not been successful. The NMR docking procedure may also be used to eliminate this problem. This procedure consists of four steps.[5,8]

1. Determine the conformation of an enzyme-bound inhibitor by NMR measurements of metal-nucleus distances and interproton distances.
2. Measure distances from a paramagnetic reference point on the enzyme (or inhibitor) to assigned proton resonances of the inhibitor (or enzyme).
3. Identify amino acid residues of the enzyme within 5 Å of the bound inhibitor by intermolecular NOEs from assigned proton resonances of the enzyme to those of the substrate.
4. Use the distances from (2) and (3) to position the proper conformation of the inhibitor into the X-ray struture of the enzyme, avoiding steric overlaps by energy minimization if necessary.

This paper makes use of the NMR docking procedure to determine the structure of the enzyme–metal–3′,5′-pdTp complex unperturbed by intermolecular interactions unique to the crystal lattice. A preliminary report of this work has been published.[9] The accompanying paper[10] provides independent support for the NMR-docked structure of the enzyme–Ca^{2+}–3′,5′-pdTp complex.

MATERIALS AND METHODS

Materials

3′,5′-pdTp was obtained from P-L Biochemicals. Ultrapure $CoCl_2$ and $CaCl_2$ were from Johnson Matthey Chemicals. Before use, all buffer and nucleotide solutions were passed over Chelex-100 resin to remove trace metals. Salmon sperm DNA, obtained from Sigma, was used in the enzyme assays following heat denaturation of the DNA for 30 min at 100°C and rapid cooling on ice.[3] The isolation and purification of wild-type staphylococcal nuclease was performed as previously described.[11,12] Enzyme concentrations were determined from the absorbance at 280 nm by using $\epsilon^{0.1\%}$ 1 cm = 0.93,[1,13,14] and staphylococcal nuclease activity was measured as previously described.[11,15]

Methods

Water proton relaxation rate measurements

The correlation times τ_c for the electron nuclear dipolar interaction in the ternary enzyme–Co^{2+}–nucleotide complexes were determined by studying the frequency dependence of $1/T_{1P}$ of water protons at 15, 24.3, 42, and 59.8 MHz on a Seimco pulsed NMR spectrometer equipped with a variable-frequency probe, at 250 MHz on a Bruker WM 250 spectrometer, and at 360 MHz on a Bruker AM 360 spectrometer by inversion recovery as previously described.[11,15] Evaluation of τ_c from the frequency-dependent $1/fT_{1P}$ values was done as described earlier.[16,17] Samples contained 40 mM TES, pH 7.4, equimolar concentrations (0.96 mM) of enzyme and 3′,5′-pdTp, and 0.81 mM $CoCl_2$ to minimize nonspecific metal binding to the enzyme. At these conditions more than 66% of the Co^{2+} was bound in the respective ternary enzyme–Co^{2+}–pdTp complex.[18] Measured dissociation constants of Co^{2+} from binary and ternary complexes[18] were used to calculate the concentrations of free and bound species in solution. The observed relaxation rates were corrected for the paramagnetic effects of free Co^{2+} in each system.

†H. B. R. Cole and D. A. Torchia (private communication, 1989).

^1H relaxation rate measurements

To measure the paramagnetic effects of enzyme-bound Co^{2+} on the relaxation rates of the carbon-bound protons of enzyme-bound 3′,5′-pdTp, a 360 μl sample was prepared which contained 627 μM staphylococcal nuclease, 6.86 mM 3′,5′-pdTp, 2.5 mM d^{11}-Tris-DCl (pH 7.4 when measured in H_2O), and 25 mM NaCl in ^2H_2O. All stock solutions were passed over Chelex 100 before use to remove paramagnetic metal ions. To remove EDTA and protonated Tris buffer from the stored enzyme, the enzyme was passed over a Sephadex G-25 column which had been equilibrated with 50 mM NaCl and 5 mM d^{11}-Tris-DCl (pH 7.4 in H_2O). The samples were deuterated by lyophilization and redissolving in ^2H_2O three times to the above final concentrations. Under these conditions 98.5% of the enzyme was in the binary enzyme–3′,5′-pdTp complex. Such solutions were then titrated with $CoCl_2$ measuring the increases in $1/T_1$ values of the protons of enzyme-bound 3′,5′-pdTp due to the paramagnetic effect of Co^{2+}. The data were analyzed by plotting the increases in the relaxation rates against the increases in the concentrations of Co^{2+} bound in the ternary complex. The slopes obtained this way, when multiplied by the total nucleotide concentration, yielded the normalized relaxation rates $1/fT_{1P}$, in which the factor f is defined as [enzyme bound metal ions]/[total nucleotide]. The normalized relaxation rates were then used in Eqs. (1) and (2) to calculate the distances r from Co^{2+} to the protons of enzyme-bound 3′,5′-pdTp, as previously described.[4,16–18]

$$r = C\{(T_{1P})_b[f(\tau_c)]\}^{1/6}. \quad (1)$$

In Eq. (1), C is a constant, equal to 895 ± 125 Å/s$^{1/3}$ for Co^{2+}–proton interactions. The correlation function is given by

$$f(\tau_c) = \frac{3\tau_c}{1 + \omega_I^2\tau_c^2} + \frac{7\tau_c}{1 + \omega_s^2\tau_c^2} \quad (2)$$

where ω_I and ω_S are the nuclear and electron precession frequencies and τ_c is the correlation time. The correlation time was determined by measuring the frequency dependence of $1/T_{1P}$ of water protons in the ternary enzyme–Co^{2+}–pdTp complex over a range of frequencies from 15 to 360 MHz. This approach is valid since the τ_c for Co^{2+} relaxation of both water and 3′,5′-pdTp protons is dominated by the short electron spin relaxation time of Co^{2+}.[18]

^1H NMR spectra were obtained at 250.13 MHz by using 16-bit A/D conversion, quadrature phase detection, a 90° observation pulse, and collecting 16 K data points over a spectral width of 2500 Hz. Fully relaxed 1D spectra were acquired by collecting 32–256 transients, using a 10 sec relaxation delay. The longitudinal relaxation rates ($1/T_1$) of ^1H resonances were measured by the nonselective saturation recovery method, which permitted shorter recycle times. Chemical shifts were relative to external DSS.

One-dimensional NOE experiments

Transferred NOE experiments at 250.13 MHz were carried out in samples containing 490 μM staphylococcal nuclease, 7.1 mM 3′,5′-pdTp, 5 mM d^{11}-Tris-DCl (pH 7.4 in H_2O), and 10 mM NaCl in ^2H_2O in the absence or presence of 1.3 mM $CaCl_2$. The samples were prepared and deuterated as described in the previous section. Spectra were collected with 16 K data points, a spectral width of 3000 Hz, an acquisition time of 2.74 sec, and 256–512 transients were collected. T_1 values were measured by the selective saturation-recovery method.[19] NOEs were generated by alternatively preirradiating on and off the resonances of interest using the pulse sequence described earlier[20,21] with a total recycle time of 4.94 sec, which was 6 times the longest T_1 value (0.82 sec), to ensure complete relaxation. Preirradiation was accomplished by using the proton decoupler, with the power set 40 dB below 0.2 W.

The time dependencies of the NOEs from each of the selectively preirradiated protons to the observed protons were fit by nonlinear regression analysis using experimentally determined NOEs and $1/T_1$ values of protons receiving NOEs as previously described[20,21] to obtain the cross relaxation rates σ_{AB}. Cross-relaxation rates resulting from the irradiation of the two unresolved H5′ and H5″ resonances of 3′,5′-pdTp or the three unresolved H5 methyl proton resonances were divided by factors of 2 and 3, respectively, to obtain relevant σ_{AB} values for distance calculations.[22] Interproton distances (r_{AB}) were then obtained from σ_{AB} using the relationship

$$r_{AB} = \left(\frac{\sigma_{std}}{\sigma_{AB}}\right)^{1/6} r_{std} \quad (3)$$

where σ_{std} is the cross relaxation rate observed for protons at a known distance (r_{std}). The known distances used were those from deoxyribose H1′ to H2″ (2.37 ± 0.1 Å) and from the thymine methyl to H6 of 3′,5′-pdTp (2.9 ± 0.1 Å) based on model building and on crystallographic studies.[4,23–25] Both of these standard distances yielded identical results, supporting the underlying assumption of Eq. (3), namely that the correlation time is the same for all interproton interactions in enzyme-bound 3′,5′-pdTp.

Two-dimensional NOE experiments

To improve resolution and to increase the signal/noise at short mixing times (τ_m), 2D NOESY spectra[26,27] were acquired at 600 MHz in addition to the 1D NOE spectra at 250 MHz. Samples contained 4.00 mM staphylococcal nuclease, 3.61 mM $CaCl_2$, 14.7 mM 3′,5′-pdTp, 30 mM NaCl, 0.04 mM EGTA,

1.4 mM Tris-DCl-d11, pH 7.4 in a total volume of 0.550 ml ^2H_2O. Samples were examined using three mixing times, 50, 100, and 200 msec, and the mixing times were varied randomly up to ± 10% to eliminate COSY cross-peaks. All spectra were acquired in the phase-sensitive mode with use of time proportional phase incrementation (TPPI).[28] Optimization of receiver phase was performed to reduce baseline roll and to minimize phase correction in F2. The parameters for acquisition of NOESY spectra included a 2.0 sec relaxation delay, an 0.254 sec acquisition time, an 8064 Hz sweep width, 4096 time domain data points in F2, 1024 time domain points in F1, and a filter width of 30 kHz. Low power presaturation (0.2 mW) of the HDO signal was applied during the relaxation delay.

Two-dimensional NOESY data were processed both on an Aspect 3000 computer with Bruker software, and on a Personal IRIS (Silicon Graphics, Inc.) utilizing the software FELIX (Hare, Inc.), with no significant differences. NMR data processed were multiplied by a $\pi/2$ shifted squared sine-bell prior to Fourier transformation in F2. Linear baseline correction in F2 was done in all cases throughout the entire spectrum. The F1 direction was Fourier transformed with zero filling to 2K points. Volume integrals of 3′,5′-pdTp cross peaks were determined as previosuly described,[4] and peak volumes were analyzed by utilizing both an initial slope method[28,29] and a distance extrapolation method,[29] using equation [3] and the reference distance $H_1' \rightarrow H_2''$ = 2.37 ± 0.1 Å to obtain interproton distances.

Modeling studies

To determine the range of conformations of metal-3′,5′-pdTp consistent with all of the measured metal-nucleus and interproton distances and their errors, a computer search procedure, D-space, was utilized (Hare Research, Inc.) as previously described.[4] A total of 75 structures were generated of which 10 were judged to be acceptable, based on their consistency with all covalent constraints, van der Waals constraints, angle constraints, and measured distances, within their experimental errors.

Docking the metal-3′,5′-pdTp complex into the X-ray structure

The structural coordinates for the enzyme-bound metal-3′,5′-pdTp complex were combined with the 1.7 Å X-ray coordinates of staphylococcal nuclease in the presence of Ca^{2+} and 3′,5′-pdTp.[7] The metal-3′,5′-pdTp complex was first manually oriented into the active site of the enzyme with the software package FRODO[30] on an Evans and Sutherland graphics system, taking into consideration the position of the metal ion, the deoxyribose rings, and the intermolecular NOE restraints from protons of 3′,5′-pdTp to assigned side-chain protons of Tyr-85, 113, and 115 of the enzyme. To relieve residual van der Waals overlaps and to optimize the structure, the manually docked enzyme-metal-3′,5′-pdTp complex was subjected to a restrained Powell energy minimization using the program X-PLOR[31] on a CONVEX C220 computer as previously described.[5] A square well effective potential function was used to represent the experimental interproton distance (NOE) restraints in addition to the full empirical energy function[31] with a force constant K_{NOE} ranging from 50 to 90 kcal mol^{-1} $Å^{-2}$. The minimization was carried out in two steps, during which the enzyme, the inhibitor 3′,5′-pdTp, and Ca^{2+} were free to move within the experimental errors of their measured intermolecular distances. In the first step, van der Waals overlaps in the manually docked enzyme–Ca^{2+}–3′,5′-pdTp structure were removed by 100 cycles of unrestrained Powell energy minimization. A hard sphere (quadratic) repulsive term was used to represent nonbonded interactions with a force constant of 4 kcal mol^{-1} $Å^{-2}$ with van der Waals radii set to 0.89 of their standard value.[31,32] The overlaps were removed within 20 cycles as evidenced by the drastic drop and negative values of the van der Waals energy which were calculated using the Lennard–Jones potential and parameters of the CHARMM empirical energy function.[33] The second step, to optimize the structure, was 2,000 cycles of restrained Powell energy minimization with the full all-hydrogen CHARMM empirical energy function with standard van der Waals radii.[31] The restraints used were the measured interproton, metal–proton, metal–phosphorus, and lower limit distances within the bound metal–3′,5′-pdTp complex, as well as measured intermolecular distances from assigned proton resonances of the enzyme to those of the bound inhibitor, taking into account their experimental errors. The planarity of the guanidiniums of Arg-35 and Arg-87 were maintained by restraining the dihedral angles Cδ–Nϵ–Cζ–Nη_1 (Nη_2) to 0 ± 2° and 180 ± 2°, respectively, and 2000 additional cycles of energy minimization were carried out. No significant changes occurred in the structure during the last 1000 cycles. To retain a heptacoordinate complex about Ca^{2+} with proper metal–ligand distances in the energy minimization, a Lennard–Jones σ value of 1.43 Å, appropriate for Ca^{2+}, and a dielectric constant of 15 were used. Recent measurements of the pK_A values of buried lysine residues indicate that a dielectric constant in the range of 10–15 is appropriate for the interior of proteins.[34,35]

To ensure that the structure was not trapped in a local minimum, 5 psec of molecular dynamics using X-PLOR was done with a time step of 1 fsec, at 300°K, with the protein backbone fixed. After the molecular dynamics run, which did not significantly change the structure, the backbone constraints were lifted and the structures underwent an additional 2000 cycles of Powell energy minimization with the

TABLE I. Distances From Co^{2+} to Protons and Phosphorus of 3',5'-pdTp in the Staphylococcal Nuclease–Co^{2+}–3',5'-pdTp Complex

Nucleus	δ (ppm)*	$1/fT_{1P}(s^{-1})^{\dagger}$	$1/fT_{2P}(s^{-1})^{\dagger}$	$r(Å)^{\dagger}$
TCH_3	1.90	3.1 ± 0.3	—	9.88 ± 2.3
TH_6	7.80	3.3 ± 0.3	—	9.80 ± 2.3
TH_1'	6.34	1.7 ± 0.2	—	11.0 ± 2.5
TH_2', H_2''	2.36, 2.49	5.3 ± 0.5	—	9.04 ± 2.1
TH_4'	4.29	10.5 ± 1.1	—	8.06 ± 1.9
TH_5', H_5''	4.00	18.4 ± 1.8	—	7.34 ± 1.7
3' P‡	4.16	82 ± 8	12,900§	4.4 ± 0.9
5' P‡	4.55	1443 ± 132	21,500§	2.7 ± 0.5

*Chemical shift ± 0.02 ppm from external DSS (protons) or from 85% H_3PO_4 in 20% ^2H_2O (phosphorus).

†$1/fT_{1P}$, $1/fT_{2P}$, and distances (r) were calculated as described in Methods. The τ_c was determined as 0.77 psec from the frequency dependence of $1/fT_{1P}$ of water protons as described in Methods. Errors in r include contributions from errors in $1/fT_{1P}$ and τ_c, and in the g value for high-spin Co^{2+} of 4 ± 2 which enters C in Eq. (1) as a cube root. The C values used are 895 ± 125 for Co^{2+}–proton distances and 662 ± 93 for Co^{2+}–^{31}P interactions.[18] Errors are shown in absolute distances, which include a 14% contribution due to the anisotropic g values of Co^{2+} and a 5–7% contribution due to experimental errors in measurements of $1/fT_{1P}$, τ_c, and thermodynamic parameters. Since the g value of Co^{2+} is the same for all of the distances, the errors in the relative distances are only 5–7%.

‡Data on the 3' P and 5' P is from Serpersu et al.[18]

§$1/T_2$ values were calculated as $\pi\Delta\nu_{1/2}$ where $\Delta\nu_{1/2}$ is the resonance width at half height. The $1/fT_{2P}$ was corrected for binary 3',5'-pdTp–Co^{2+} contributions.[18] Since $1/fT_{2P} >> 1/fT_{1P}$, fast exchange assumptions are valid, permitting the use of Eq. (1) for distance calculations.[16]

same parameters as described above, again with little change in structure.

RESULTS AND DISCUSSION

Paramagnetic Effects of Co^{2+} on the Longitudinal Relaxation Rates of Protons of Enzyme Bound 3',5'-pdTp

We have previously reported paramagnetic effects of Co^{2+} on the longitudinal ($1/fT_{1P}$) and transverse ($1/fT_{2P}$) relaxation rates of the phosphorus nuclei of 3',5'-pdTp and Co^{2+} to phorphorus distances in the ternary staphylococcal nuclease–Co^{2+}-3',5'-pdTp complex (Table I).[18] To determine the conformation of enzyme-bound 3',5'-pdTp, metal to proton distances are also necessary. Figure 1A shows the proton NMR spectrum at 250 MHz of 3',5'-pdTp in the presence of the enzyme and Figure 1B and C shows the paramagnetic effects of enzyme-bound Co^{2+} on $1/T_1$ of the protons of 3',5'-pdTp. Table I summarizes the normalized longitudinal relaxation rates ($1/fT_{1P}$) of the protons of 3',5'-pdTp corrected for the small effects of free Co^{2+} as measured in a separate titration of 3',5'-pdTp with Co^{2+} in the absence of enzyme. The $1/fT_{1P}$ values for the protons of enzyme-bound 3',5'-pdTp are much smaller than the $1/fT_{1P}$ and $1/fT_{2P}$ values of the phosphorus nuclei (Table I), indicating that the proton relaxation rates are in the fast exchange case and suitable for distance determinations. The correlation time for the Co^{2+}–proton dipolar interaction, determined by the frequency dependence of $1/T_{1P}$ of water protons in the same complex, as described in Methods, was found to be 0.77×10^{-12} sec, a typical value for the electron spin relaxation time of high-spin Co^{2+}.[4,16,18] Distances from enzyme-bound Co^{2+} to the protons of 3',5'-pdTp, calculated with Eqs. (1) and (2), are given in Table I, together with previously determined Co^{2+} to phosphorus distances in the same complex. These distances were mutually consistent in that they could be used to manually construct stick models of the conformation of enzyme-bound Co^{2+}–3',5'-pdTp in which all of the metal–nucleus distances converged, within experimental error, to a single point at the metal. However, two such conformations consistent with the metal–nucleus distances were found, one with a low-anti conformation about the glycosidic bond, and the other with a syn conformation. The predicted interproton distances in these two conformations differed significantly, indicating that NOE studies could be used to resolve this ambiguity.

Studies of Conformation of Enzyme-Bound 3',5'-pdTp Using Intramolecular Nuclear Overhauser Effects

Nuclear Overhauser effects (NOEs) can be used to determine interproton distances of ≤4 Å[22] and can, therefore, in fast exchanging systems yield further information on the conformation of an enzyme-bound nucleotide.[4,20,21,36] Such 1D NOE studies were carried out at 0.49 mM enzyme, 7.1 mM 3',5'-pdTp, in the presence of 1.3 mM $CaCl_2$. At the end of these experiments which, usually lasted 5–6 days, the enzyme retained more than 95% of its original activity. Intramolecular NOEs on bound 3',5'-pdTp were measured by selectively preirradiating the H1', H2', H2", H3', H4', H5',5", H6, and H5 (methyl) protons and observing changes in the magnetization of the nonirradiated 3',5'-pdTp resonances. The H3' resonance was obscured by the large HDO signal. Therefore, its position was determined by decoupling experiments which were performed simply by searching for a frequency which would decouple the H4' resonance from that of H3'.

The length of preirradiation was systematically varied in order to observe the time course of the development of NOEs. This approach allowed discrimination between primary and secondary effects, since the latter show a long lag period before the development of negative NOEs. From the negative NOEs, cross-relaxation rates (σ_{AB}) were determined and interproton distances were calculated with Eq. (3) as described in Materials and Methods using the σ_{std} values determined from H2" to H1' and the interproton distance of 2.37 ± 0.1 Å as a reference standard.[25] Using this approach, the calculated dis-

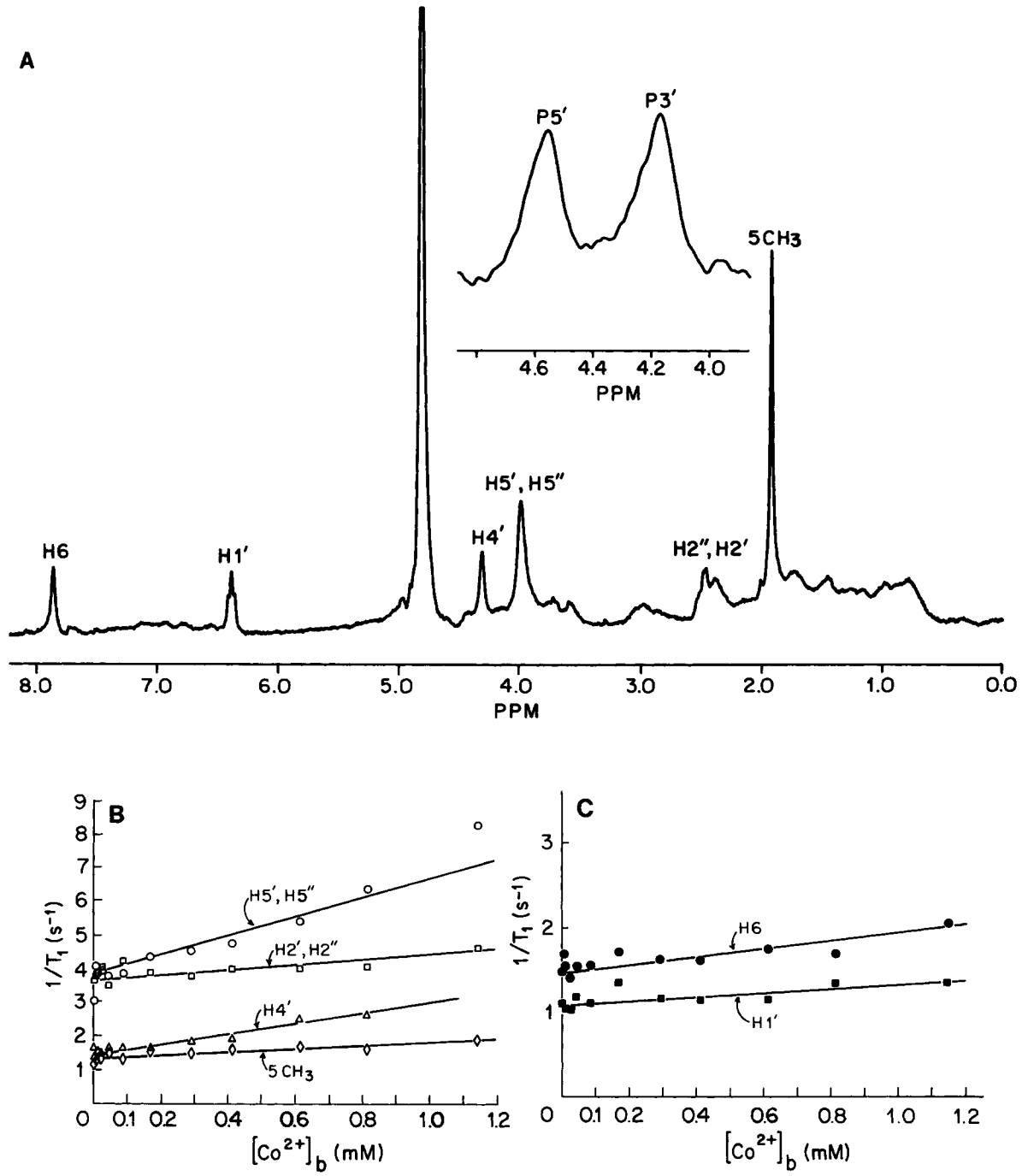

Fig. 1. ^{1}H and ^{31}P NMR spectra of the inhibitor 3',5'-pdTp and paramagnetic effects of Co^{2+} on the $1/T_1$ of the protons of 3',5'-pdTp in the presence of staphylococcal nuclease. **(A)** 250 MHz protons and (inset) 101.25 MHz proton decoupled phosphorus NMR spectrum in the presence of wild-type staphylococcal nuclease. In **(B)** paramagnetic effects of Co^{2+} on the protons H5'H5" (○), H2'H2" (□), H4' (△), and 5 CH_3 (◇) are shown together with those in **(C)** for the H_6 (●) and H_1' (■) protons. Conditions and the sample are described in Methods, and in all experiments greater than 95% of the enzyme was in the binary enzyme-3',5'-pdTp complex at the beginning of the titration.

tance from the H6 to the H5 methyl protons of bound 3',5'-pdTp was found to be 2.87 ± 0.19 Å, consistent with its known value of 2.93 ± 0.1 Å and the calculated distance from H1' to H2' was 2.73 ± 0.16 Å, consistent with its known range of values of 2.9 ± 0.2 Å (Table II).[20,21]

The NOEs determined by 1D methods at 250 MHz showed relatively low signal/noise, necessitating

TABLE II. Interproton Distances in Angstrom Units Calculated From 1D and 2D NOE Experiments in Ternary Enzyme–Metal–3′,5′-pdTp and Binary Enzyme–3′,5′-pdTp Complexes of Staphylococcal Nuclease

Proton pair	Ternary E–Metal–3′,5′-pdTp complex				Binary E–3′,5′-pdTp complex
	2D NOESY volume integration				
B ↔ A*	Method 1 (initial slope)	Method 2 (*r* vs. mixing time)	Average	1D presaturation area integration	1D presaturation area integration
$H_1' \leftrightarrow H_4'$	3.20 ± 1.06	3.90 ± 0.80	3.55 ± 1.32	—	—
$H_1' \leftrightarrow H_2''$†	2.37 ± 0.10	2.37 ± 0.10	2.37 ± 0.10	2.37 ± 0.10	2.37 ± 0.10
$H_1' \leftrightarrow H_2'$‡	2.82 ± 0.16	3.09 ± 0.35	2.96 ± 0.38	2.73 ± 0.16	2.74 ± 0.10
$H_6 \leftrightarrow H_1'$	3.65 ± 0.10	3.98 ± 0.34	3.82 ± 0.35	—	—
$H_6 \leftrightarrow H_4'$	3.83 ± 0.53	4.40 ± 0.20	4.12 ± 0.57	—	—
$H_6 \leftrightarrow H_5'H_5''$	2.87 ± 0.08	2.82 ± 0.32	2.84 ± 0.33	2.61 ± 0.07	2.55 ± 0.08
$H_6 \leftrightarrow H_2'$	2.76 ± 0.31	2.95 ± 0.39	2.86 ± 0.50	—	—
$H_6 \leftrightarrow H_2''$	3.07 ± 0.33	3.32 ± 0.50	3.20 ± 0.60	—	—
$H_6 \leftrightarrow TCH_3$§	2.87 ± 0.16	2.83 ± 0.07	2.85 ± 0.17	2.87 ± 0.19	2.82 ± 0.09
$H_3' \rightarrow H_5'H_5''$	**	**	**	2.42 ± 0.13††	2.54 ± 0.15††

*B ↔ A represents an NOE occurring between the protons A and B as measured in both columns and rows of a two-dimensional NOESY. For a one-dimensional experiment, B ↔ A represents the average of distances measured by preirradiation of both A and B and observing NOEs to B and A, respectively, for all cases except for the proton pair $H_3' \rightarrow H_5',H_5''$ where only the indicated direction could be studied (see footnote ††).

†Reference distance assumed to be 2.37 ± 0.1 Å based on X-ray data and model building of nucleotides.[4,25]

‡Expected value is 2.9 ± 0.2 Å based on X-ray data and model building[20] providing an internal check of the measured interproton distances.

§Expected value of 2.9 ± 0.1 Å based on X-ray structure and model building[4] providing a second internal check of the interproton distances.

**NOESY cross peak obscured by HDO signal.

†† From 1D NOEs detected after preirradiation of H_3' under the HDO resonance which was located by underwater decoupling. The reverse experiment could not be done.

long preirradiation times (150 to 1200 msec). Because of the possible effects of spin diffusion, the interproton NOEs were independently determined with greater sensitivity and resolution and at short mixing times (50–200 msec) by 2D methods at 600 MHz (Fig. 2). The NOE data for the enzyme–Ca^{2+}–3′,5′-pdTp complex were analyzed by the initial slope method and by the distance vs. mixing time method with very similar results (Table II). The interproton distances obtained by 2D methods at 600 MHz agreed within error with those measured by the 1D presaturation method at 250 MHz. With the higher resolution and improved sensitivity at 600 MHz, additional interproton distances could be obtained (Table II). Interestingly, within error, the same interproton distances in 3′,5′-pdTp are found in the binary enzyme-nucleotide complex (Table II).

Conformation of Enzyme Bound 3′,5′-pdTp

Using the 8 measured Co^{2+}–nucleus distances (Table I) together with the 9 measured (Table II) and 45 lower limit interproton distances (i.e., proton pairs between which NOEs were not observed),‡ a structural model of the conformation of 3′,5′-pdTp in the ternary enzyme–metal–inhibitor complex was computed. The distance geometry program D-space, which takes into account the experimental distances and their errors as well as van der Waal radii of the atoms of 3′,5′-pdTp, was utilized to perform 75 conformational searches, each starting from randomized coordinates. These searches led to ten structures which satisfied the experimental distances and the van der Waals constraints with a total deviation ≤ 0.46 Å. These structures were all very similar (Fig. 3A), with the two most different structures having a root mean square difference for all atoms of 0.79 Å, while the average root mean square difference for all pairs of structures was 0.52 Å, indicating that they represented a single conformation.

The conformational angles for 3′,5′-pdTp bound to staphylococcal nuclease in the presence of metal ions (Fig. 3A) are summarized in Table III and are compared with those found in the 1.7 Å X-ray structure of the staphylococcal nuclease–Ca^{2+}–3′,5′-pdTp complex (Fig. 3B).[7] For the torsional angles δ, ε, and χ no detectable changes were observed when the NMR and X-ray structures of enzyme-bound 3′,5′-pdTp are compared, while the angle β changes from each of the two possible orientations found in the NMR structure. The major difference between the two structures results from a 115 ± 31° difference in the torsional angle γ about the C4′–C5′ bond resulting in a trans, gauche conformation in the

‡The use of lower limit distances did not significantly change the conformation of enzyme-bound 3′,5′-pdTp.

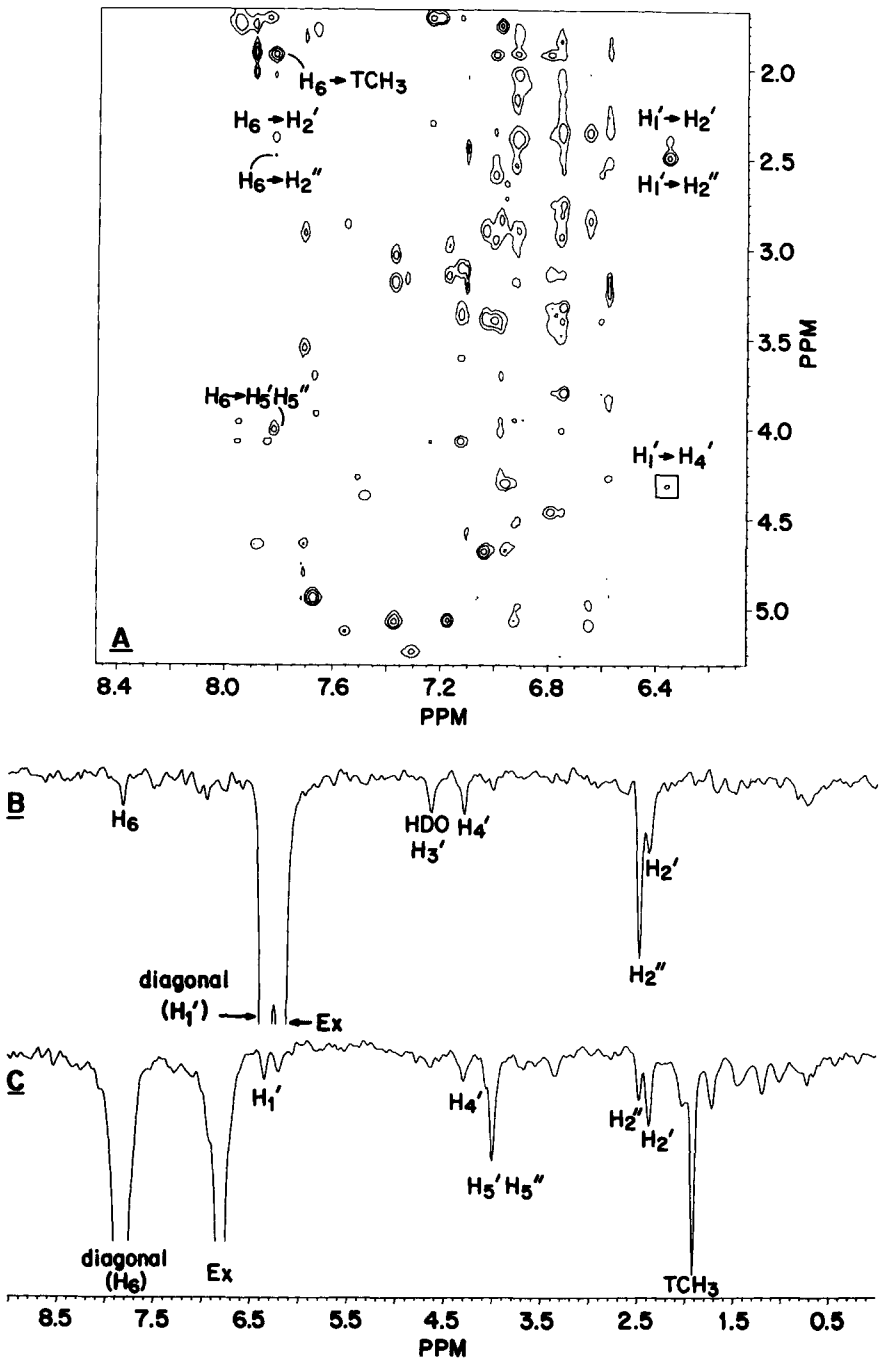

Fig. 2. Two-dimensional nuclear overhauser effect (NOESY) spectra at 600 MHz of the enzyme-Ca^{2+}-3',5'-pdTp ternary complex of wild-type staphylococcal nuclease. **(A)** Two-dimensional display of a 50 msec NOESY spectrum of the enzyme–Ca^{2+}–3',5'-pdTp complex. The intensity of the boxed cross peak showing an NOE from H1' to H4' has been multiplied by 2 to make it more visible. Representative columns [in the F1 dimension of **(A)**] arising from **(B)** the H_1' proton resonance (6.34 ppm) and **(C)** the H_6 proton resonance (7.80 ppm) of 3',5'-pdTp show the magnitude of the NOE intensities and the signal to noise ratio of the data. Peaks labeled Ex are exchange peaks[37,44] arising from the slow exchange of Ca^{2+} which interconverts binary enzyme–pdTp and ternary enzyme–Ca^{2+}–pdTp complexes. On saturation with Ca^{2+} (30 mM), these exchange cross peaks disappear. Conditions and sample are described in Methods.

NMR determined structure and a gauche, trans conformation in the X-ray structure. This discrepancy arises from an artifact in the X-ray structure due to crystal packing in which Lys-70* and Lys-71* from an adjacent molecule of staphylococcal nuclease in the crystal lattice are inserted into the active site. Notably, Lys-70* is positioned between the 3'- and 5'-phosphates of 3',5'-pdTp resulting in a 6.31 ± 0.2

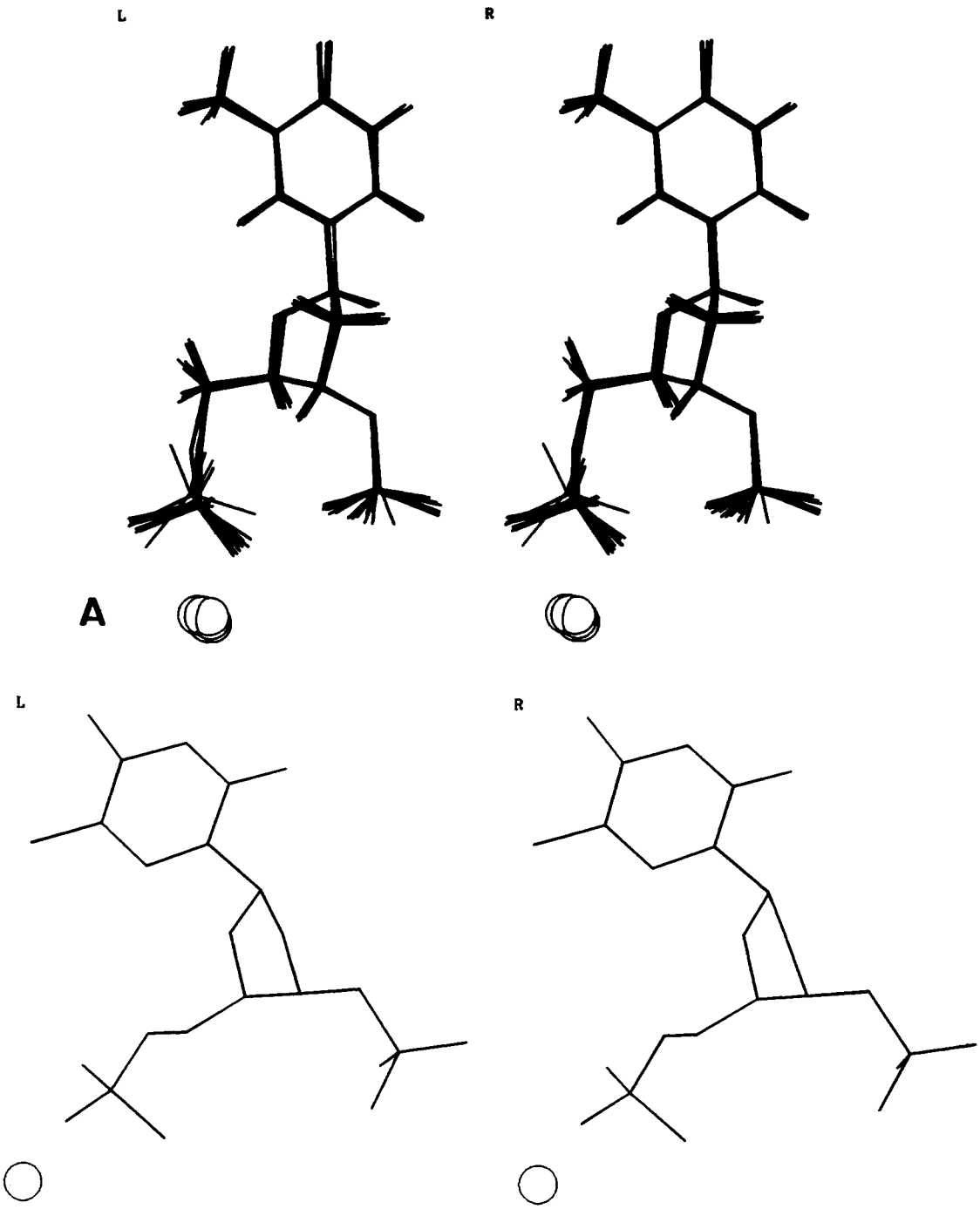

Fig. 3. Conformations of enzyme-bound 3′,5′-pdTp in the presence of metal ion based on NMR and X-ray crystallography. **(A)** Comparison of 10 acceptable structures of 3′,5′-pdTp each with deviations from the NMR-determined distances of Tables I and II, from known bond lengths and geometries, and from van der Waals constraints totalling to ≤0.46 Å. The root mean square difference between the two most different structures is 0.79 Å, while the average root mean square difference for all pairs of structures is 0.52 Å. **(B)** Conformation of enzyme-bound 3′,5′-pdTp determined by X-ray crystallography.[7]

Å distance between the 3′- and 5′-phosphorus atoms.[7] In the NMR structure, no such distortion of enzyme-bound 3′,5′-pdTp exists and the phosphorus atoms are 1.9 Å closer, separated by only 4.1 ± 0.8 Å. Another manifestation of this artifact of crystal packing, as previously noted,[6,18] is the 5.4 Å greater distance from the metal to the 3′-phosphorus of 3′,5′-pdTp in the crystal structure (9.82 ± 0.2 Å) in comparison with the solution structure (4.4 ± 0.9 Å) (Table I). In both the crystal and solution structures,

TABLE III. Comparison of Torsional Angles of Enzyme-Bound 3′,5′-pdTp in the Enzyme–Metal–3′,5′-pdTp Ternary Complex as Determined by X-Ray Crystallography and NMR

Torsional angle*	NMR†	X-ray‡
β	92 ± 8°	136 ± 10°
	274 ± 3°	
γ	301 ± 29°	186 ± 12°
δ	143 ± 2°	150 ± 7°
ε	273 ± 4°	267 ± 10°
χ	58 ± 10°	40 ± 8°

*Torsional angles are defined as follows:[24,43] β, P–O5′–C5′–C4′;γ, O5′–C5′–C4′–C3′;δ, C5′–C4′–C3′–O3′;ε, C4′–C3′–O3′–P;χ, O4′–C1′–N1–C6.

†Errors estimated from the range of dihedral angles found in the 10 acceptable structures of enzyme-bound 3′,5′-pdTp determined by NMR (Fig. 3A).

‡Errors estimated from the range of dihedral angles of 3′,5′-pdTp found on wild-type staphylococcal nuclease and on three highly refined isomorphous crystal structures of mutants remote from the active site.

the 5′-phosphate of 3′,5′-pdTp is directly coordinated by the metal.

Since only four interproton distances were obtained for 3′,5′-pdTp in the binary enzyme–inhibitor complex (Table II), the complete conformation of 3′,5′-pdTp in this complex could not be determined. However, these distances are indistinguishable from those found in the ternary enzyme–metal–3′,5′-pdTp complex suggesting similar nucleotide conformations both in the presence and absence of metal. This result differs from that found with the enzyme-bound substrate dTdA where the presence of the metal altered the conformation of the leaving dA moiety.[4]

Intermolecular Nuclear Overhauser Effects Between Enzyme-Bound 3′,5′-pdTp and Staphylococcal Nuclease

NOESY spectra of the staphylococcal nuclease–Ca^{2+}–3′,5′-pdTp complex obtained with mixing times of 50, 100, and 200 msec (Fig. 4) reveal intramolecular NOEs within the bound inhibitor (as discussed above), and within the protein as previously assigned.[5,37,38] In addition, at all mixing times, unique intermolecular NOEs between sequence specifically assigned aromatic proton resonances of Tyr-85, 113, and 115 and protons of 3′,5′-pdTp were detected (Fig. 4), and are summarized in Table IV. These intermolecular NOEs, which result from active site binding of 3′,5′-pdTp, were used for positioning the metal–inhibitor complex in the X-ray structure of the enzyme.

NMR Docking of Metal–3′,5′-pdTp Complex Into the X-Ray Structure of Staphylococcal Nuclease

The NMR-determined conformation of the metal–3′,5′-pdTp complex was manually docked into the X-ray structure of the staphylococcal nuclease–Ca^{2+}–3′,5′-pdTp complex, initially superimposing the metal ions and the deoxyribose rings, taking

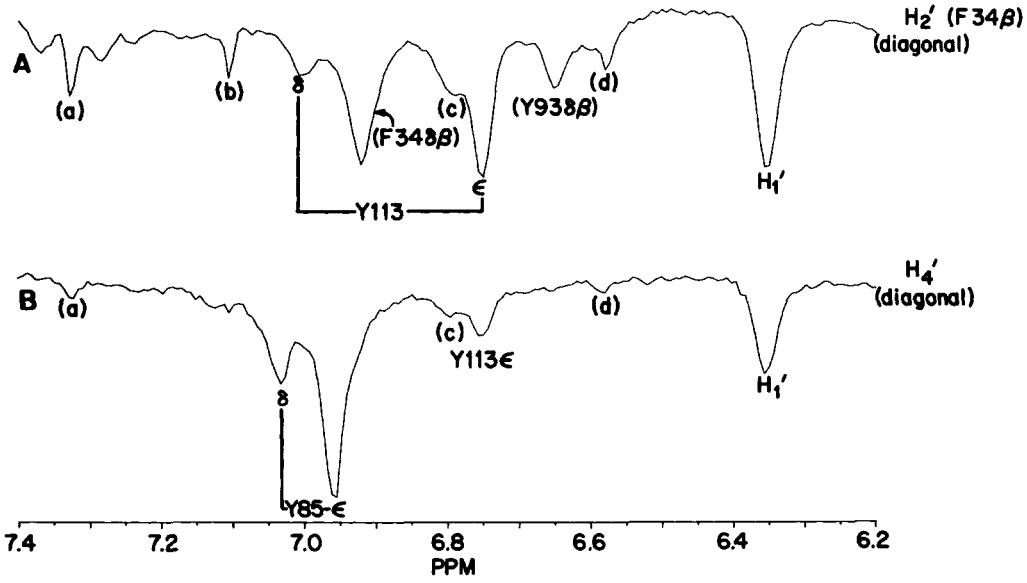

Fig. 4. Intermolecular NOEs between protons of staphylococcal nuclease and protons of 3′,5′-pdTp. Representative rows (in the F2 dimension) from the ^1H NOESY spectrum of the ternary staphylococcal nuclease–Ca^{2+}–3′,5′-pdTp complex in ^2H_2O, pD = 7.0 at 600 MHz, with a mixing time of 200 msec, showing NOEs from **(A)** the H_2' proton resonance (2.36 ppm), and **(B)** the H_4' proton resonance (4.29 ppm) to protons of 3′,5′-pdTp. Assignments are based on chemical shift data.[5,37,38] Intraprotein NOEs are labeled in parentheses. The peaks labeled (a) through (d) are intraprotein NOEs from unassigned proton resonances of the enzyme to those of Y27δ, F61δ, Y54δ, and Y91ε, respectively. All other experimental conditions and concentrations are given in Methods.

TABLE IV. Intermolecular NOEs From Protons of the Enzyme-Bound Inhibitor, 3′,5′-pdTp, to Tyrosine Protons of Staphylococcal Nuclease in the Enzyme–Ca^{2+}–pdTp Ternary Complex

		Intermolecular NOE to enzyme		
3′,5′-pdTp proton	Chemical shift (ppm)	Chemical shift (ppm)	Magnitude*	Assignment†
H_1'	6.34	6.96	Weak	85ϵ
		7.03	Weak	85δ
		6.75	Weak	113ϵ
H_2'	2.36	6.75	Medium	113ϵ
		7.00	Weak	113δ
		6.58	Weak	115ϵ
H_2''	2.49	6.96	Weak	85ϵ
		6.75	Medium	113ϵ
		7.00	Weak	113δ
		6.59	Weak	115ϵ
		7.17	Weak	115δ
H_4'	4.29	6.96	Strong–medium	85ϵ
		7.03	Weak	85δ
$H_5'H_5''$	4.00	6.96	Weak	85ϵ
		6.75	Weak	113ϵ
TCH_3	1.90	6.75	Weak	113ϵ
		7.00	Weak	113δ
		6.59	Weak	115ϵ
		7.11	Weak	115δ

*Strong, medium, and weak NOEs were assigned distances of 2.0–3.0, 3.0–4.0, and 4.0–6.0 Å, respectively.
†Intermolecular NOE assignments were based on chemical shift data.[5,37,38]

into account the intermolecular NOEs between protons of the inhibitor and those of Tyr-85, 113, and 115 (Table IV) (Fig. 5A). The manually docked structure satisfied the intermolecular NOE distance constraints, yet retained some small van der Waals overlaps. To remove these overlaps and to optimize the position of the bound metal–3′,5′-pdTp complex, energy minimization was necessary. The final energy minimized structure, the parameters of which are summarized in Table V, successfully eliminated the van der Waals overlaps and showed only minor deviations from ideal bond lengths, angles, and planarities and from the 8 experimentally determined Co^{2+} nucleus distances (Table I), the 9 experimentally determined intramolecular interproton distances (Table II), and the 19 intermolecular proximities detected experimentally (Table IV).[§] Table VI lists all violations of the experimentally determined distances and proximities from Tables I, II, and IV in the NMR docked structure and in the original X-ray structure. Clearly the NMR-docked structure provides a much better fit to the experimental data obtained in solution than does the X-ray structure. The NMR docking procedure resulted in little change in the structure of the protein. Thus the RMSD of all atoms of the NMR docked structure from those of the X-ray structure was 1.21 Å and for backbone atoms was only 0.70 Å. As a result of the intermolecular NOEs and the altered structure of 3′,5′-pdTp, small conformational changes were found in the side chains of Tyr-113 ($\Delta\chi_2 = 41 \pm 14°$) and Tyr-115 ($\Delta\chi_1 = -48 \pm 14°$; $\Delta\chi_2 = -42 \pm 14°$).

Examination of the resulting NMR docked structure (Figs. 5B, 6, 7) revealed several differences from those previously found by X-ray crystallography alone.[7] While the two structures of 3′,5′-pdTp overlapped at the metal-coordinated 5′-phosphate, the orientations of the base, deoxyribose, and 3′-phosphate were significantly altered (Fig. 5B). The altered position of the thymine ring in the NMR-docked structure places N3 in hydrogen bonding distance (3.16 Å) from the phenolic oxygen of Tyr-115. This interaction, which was not observed in the X-ray structure (5.28 Å), is supported by mutagenesis studies which reveal no loss of activity and a 3.6

[§]Although structures of the metal-3′,5′-pdTp complex with both β values (Table III) were docked into the X-ray structure, and energy minimized, the nucleotide conformation with $\beta = 92 \pm 8°$ is preferred, for two reasons. First, this angle is much closer to that found by X-ray ($136 \pm 10°$, Table III).[7] Second, the alternative β-value of $274 \pm 3°$ leads to interactions of Arg-35 and Arg-87 with the 5′-phosphate of pdTp which differ from those found in the X-ray structure[7] and in the NMR docked structure of the enzyme–metal–dTdA substrate complex.[5] Thus, to minimize differences from the X-ray structure, the conservative choice of $\beta = 92 \pm 8°$ for 3′,5′-pdTp was made and is shown.

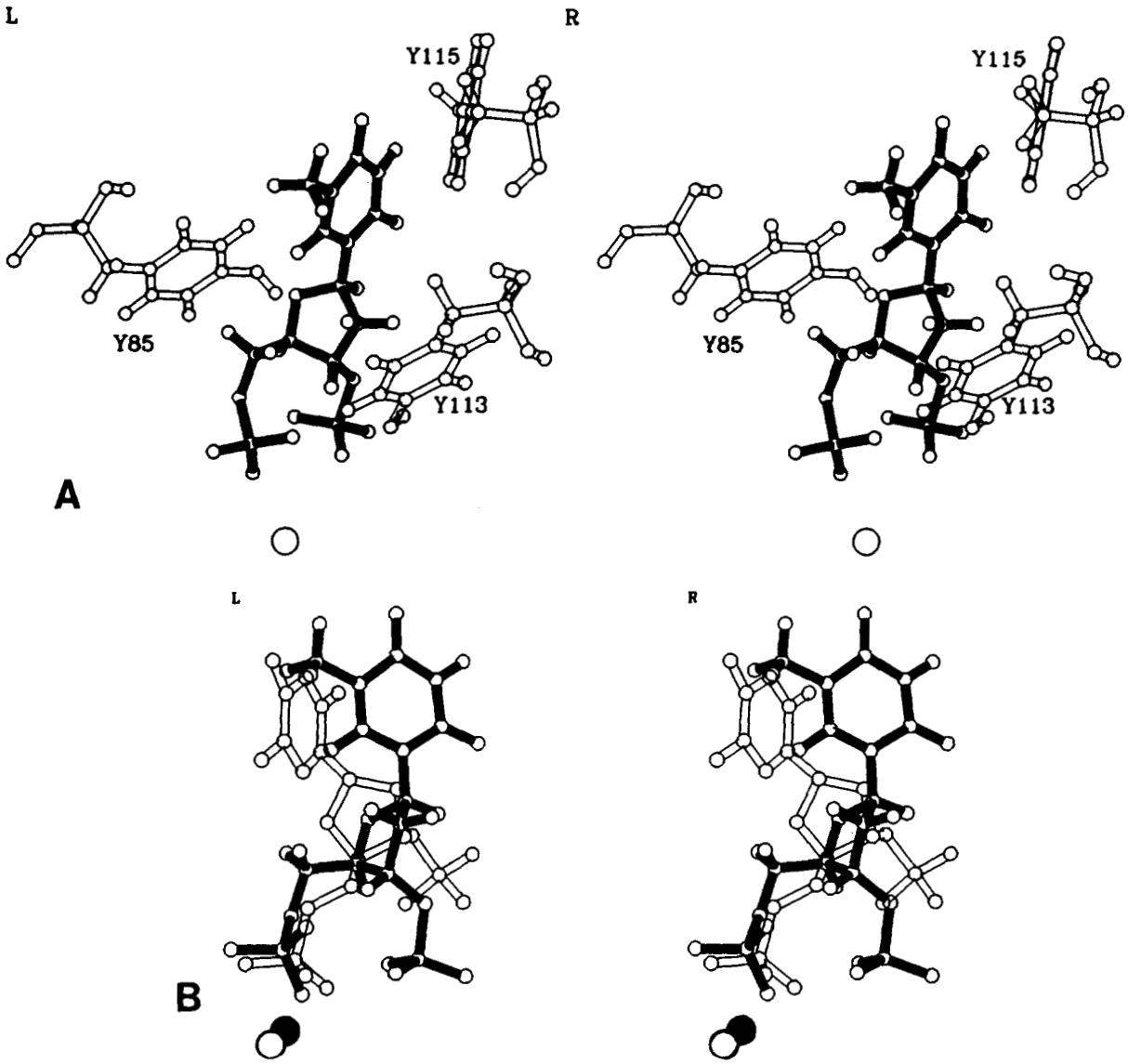

Fig. 5. Conformation and location of the inhibitor 3′,5′-pdTp docked into the X-ray structure of staphylococcal nuclease. **(A)** Protons of the tyrosine residues displayed (open) show intermolecular NOEs to protons of 3′,5′-pdTp (filled) (Table IV), and show change in chemical shifts when a substrate, dTdA, is displaced by the inhibitor.[5] **(B)** Superposition of NMR-docked conformation of 3′,5′-pdTp (filled) and conformation determined from X-ray structure of ternary enzyme-Ca^{2+}-3′,5′-pdTp complex (open).[7]

± 1.6-fold lower affinity of 3′,5′-pdTp for the Y115A mutant than for the wild-type enzyme.[10]

Another difference in the NMR-docked structure that is likely due to the absence of the lattice interactions with Lys-70* and 71* from a neighboring molecule of staphylococcal nuclease, is the location of the 3′-phosphate of bound 3′,5′-pdTp (Fig. 6). While in the X-ray structure the 3′-phosphate of the inhibitor is hydrogen bonded by both Lys-84 and Tyr-85, distances in the NMR-docked structure are too great for these hydrogen bonds to be made (8.63 Å, 4.85 Å). Instead, a hydrogen bond to the 3′-phosphate from Lys-49 (2.89 Å) is found (Fig. 6). Consistent with the NMR-docked structure, the fully active K49A mutant enzyme shows a 4.4 ± 1.8-fold weaker binding of 3′,5′-pdTp than does the wild-type enzyme, while the K84A mutant shows no significant change (1.5 ± 0.7-fold) in the binding of this inhibitor.[10] Similarly, deletion of residues 44 to 49 from the active site of staphylococcal nuclease results in a 2.4-fold decrease in affinity for 3′,5′-pdTp.[39] The weakness of the hydrogen bond from Lys-49 to the 3′-phosphate may result from mobility of the omega loop in which Lys-49 is found. It should

TABLE V. Average Deviations From Ideality and Energies of Staphylococcal Nuclease–Ca^{2+}-3′,5′-pdTp Docked Structure

Potential energy function	
E_{NOE}* (kcal/mol)	0.564
E_{VDW}† (kcal/mol)	−644.839
Deviations from ideality (RMSD)	
Bond lengths (Å)	0.01
Bond angles (deg)	2.40
Impropers‡ (deg)	0.12

*Utilizing the force constant 90 kcal/mol/Å^2.
†Utilizing the CHARMM parameters[33] for the Lennard–Jones potential.
‡Deviations from planarity in aromatic ring systems and peptide bonds.

be noted that this deletion mutant is 140- to 187-fold less active than the wild-type enzyme based on its k_{cat}/K_M values. Hence it may well interact differently with 3′,5′-pdTp. Also consistent with the NMR-docked structure, is a kinetic study of the Y85F mutant of staphylococcal nuclease[40] which showed no significant changes in the K_M values of the substrates thymidine-3′-phosphate-5′-(*p*-nitrophenyl phosphate) or thymidine-3′-methyl phosphonate-5′-(*p*-nitrophenyl phosphate) from those obtained with the wild-type enzyme. The former substrate, however, showed a 14-fold decrease in k_{cat} with the Y85F mutant enzyme, suggesting an interaction between Tyr-85 and the 3′-phosphate at a later stage of the reaction subsequent to binding.

In the NMR-docked structures of both the substrate complex,[5] and the inhibitor complex (Fig. 7) an adjacent water ligand on the metal is optimally positioned to attack the coordinated phosphate with inversion, with Glu-43 functioning as the general base. In the X-ray structure of the inhibitor complex, only a second-sphere water ligand, a less likely candidate to be the attacking water, is near enough to Glu-43 to donate a hydrogen bond to this residue,[7,41] presumably due to the interaction of Lys-71* from an adjacent enzyme molecule in the crystal lattice with Glu-43.

In both the NMR-docked and X-ray structures of the enzyme–metal-·3′,5′-pdTp complex, Arg-35 and Arg-87 serve as bifunctional hydrogen bond donors to the coordinated 5′-phosphate (Fig. 7), with Arg-87 hydrogen bonded to O5′ and therefore probably functioning as the general acid catalyst. Because of the extra negative charge on the coordinated 5′-phosphate of 3′,5′-pdTp in comparison with that of a phosphodiester substrate such as dTdA, the former may be considered to approximate a transition state analog. This view is supported by the observation that 3′,5′-pdTp binds to the enzyme–Ca^{2+} complex

TABLE VI. Deviations From Experimental Distances (in Angstrom Units) in NMR Docked and X-Ray Structures*

Distance	Experimental	NMR docking	Δ	X-ray	Δ
Intramolecular					
Co^{2+} to TH_6	9.8 ± 2.3	8.77	—	7.08	0.42
3′ P	4.4 ± 0.9	5.30	—	9.82	4.52
5′ P	2.7 ± 0.5	3.20	—	3.93	0.73
TH_6 to $TH_{2''}$	3.2 ± 0.6	3.84	0.04	4.23	0.43
$TH_{5'5''}$†	2.84 ± 0.33	3.28	0.11	2.31	0.20
$TH_{3'}$ to $TH_{5'5''}$†	2.42 ± 0.13	2.64	0.09	2.67	0.12
Sum of intramolecular deviations			0.24		6.42
Intermolecular					
$H_{1'}$ to Y85ε‡	5.0 ± 1.0	4.41	—	3.76	0.24
Y113δ‡	5.0 ± 1.0	6.15	0.15	5.80	—
$H_{2'}$ to Y115ε‡	5.0 ± 1.0	5.48	—	3.86	0.14
$H_{2''}$ to Y115δ‡	5.0 ± 1.0	6.03	0.03	5.79	—
$H_{5'5''}$ to Y113ε§	5.0 ± 1.0	4.26	—	3.87	0.13
Sum of intermolecular deviations			0.18		0.51
Total deviations (intra + intermolecular)			0.42		6.93

*Deviations (Δ) are calculated by subtracting distances found in the NMR docked or X-ray structures from the appropriate limits of the experimental distances, except as indicated, when two unresolved protons are involved.
†Deviations (Δ) are calculated by subtracting $\langle r \rangle$, the root mean sixth average value [obtained by $1/\langle r \rangle^6 = 0.5/(r \text{ to } H_{5'})^6 + 0.5/(r \text{ to } H_{5''})^6$], found in the NMR docked and X-ray structures from the appropriate limits of the experimental distances.
‡Deviations (Δ) are calculated as described in footnote † and also by subtracting the distance of the closest Tyrδ or ε proton from the appropriate limits of the experimental distances. The smaller of the two deviations thus calculated is given.
§Deviation (Δ) is calculated as in footnote ‡, except that $\langle r \rangle$ is obtained by $1/\langle r \rangle^6 = 0.25/(r\varepsilon_1 \text{ to } H_{5'})^6 + 0.25/(r\varepsilon_1 \text{ to } H_{5''})^6 + 0.25/(r\varepsilon_2 \text{ to } H_{5'})^6 + 0.25/(r\varepsilon_2 \text{ to } H_{5''})^6$.

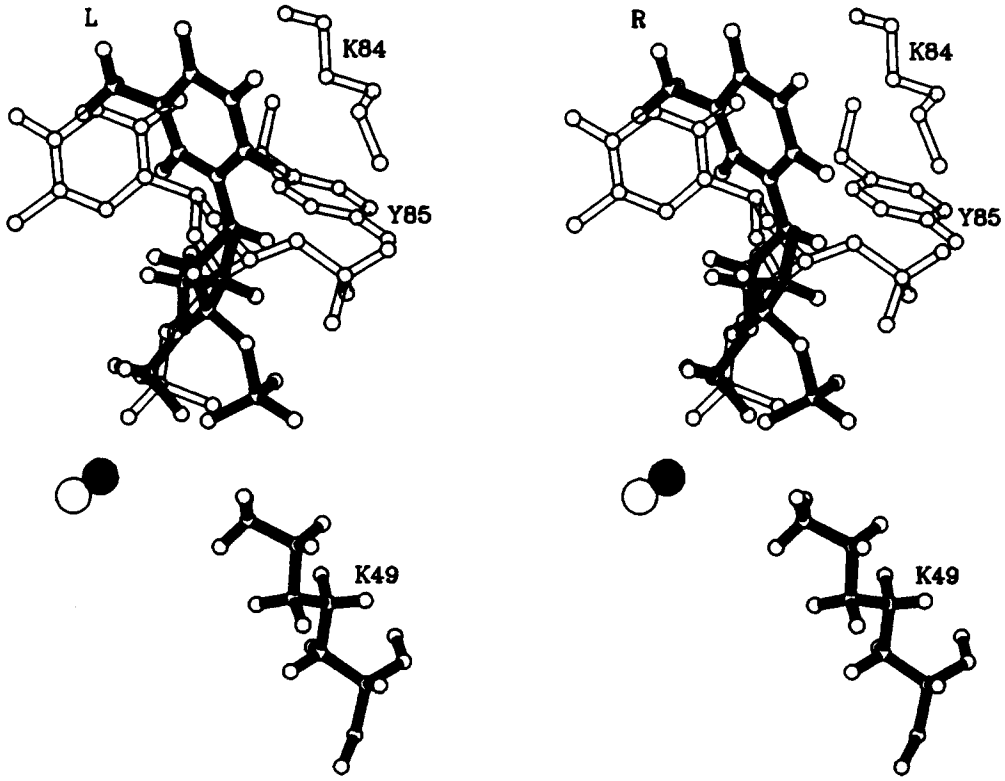

Fig. 6. Comparison of locations and interactions of enzyme-bound 3′,5′-pdTp in the presence of metal ion as determined by NMR docking (filled) and X-ray crystallography (open) showing differing interactions of the 3′-phosphate of the inhibitor.

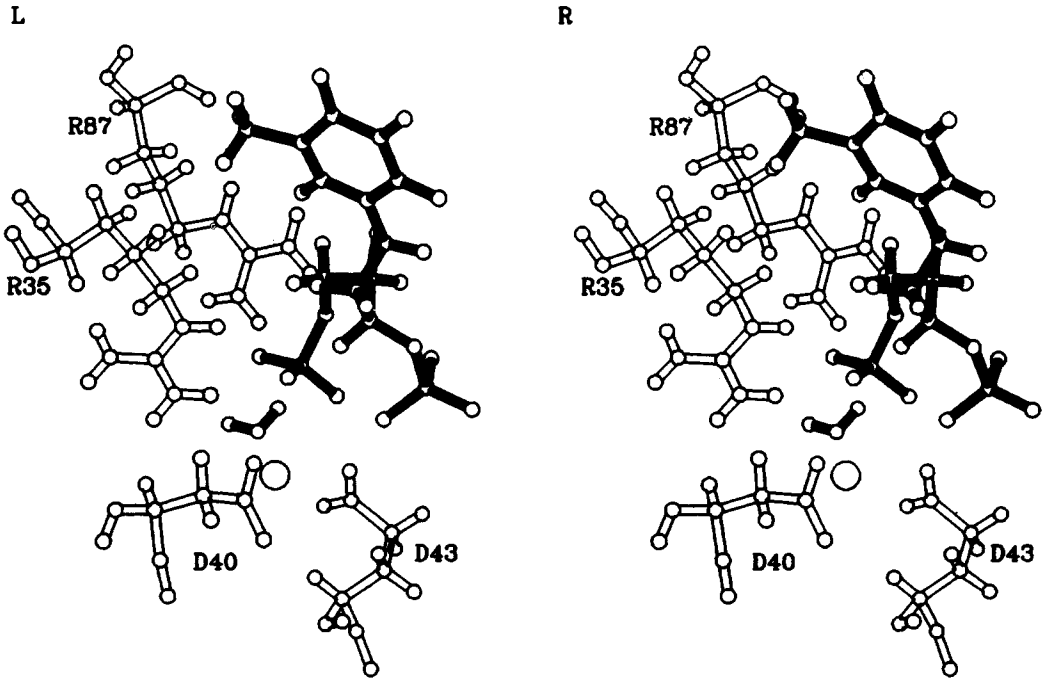

Fig. 7. NMR-docked structure of enzyme-bound 3′,5′-pdTp (filled) together with the metal ion and catalytic residues (open). Also shown is the likely attacking water molecule (filled).

1400-fold more tightly than does the substrate dTdA.[4] This greater affinity may result not only from the greater charge of the inhibitor, but also from bidentate hydrogen bond donation from both Arg-35 and Arg-87 to the 5′-phosphate of 3′,5′-pdTp, while only monodentate hydrogen bonds to the phosphodiester of the substrate were found.[5] Such a change from monodentate to bidentate hydrogen bonding as the substrate proceeds from the ground state to the transition state is supported by mutagenesis experiments which reveal that Arg to Lys mutations at positions 35 and 87 result in 10^4- to 10^5-fold decreases in catalysis,[42] comparable in magnitude to the effects of Gly substitutions at these positions.[15] Thus, Lys which can serve only as a monodentate hydrogen bond donor is ineffective at these positions.

CONCLUSIONS

NMR docking of the metal–3′,5′-pdTp complex in a conformation determined on the enzyme in solution, and therefore unperturbed by crystal lattice artifacts, into the X-ray structure of staphylococcal nuclease, together with energy minimization, has provided a deeper understanding of the structure of this complex which may serve as a model of the transition state. While the 5′-phosphate remains coordinated by the metal and receives bifunctional hydrogen bonds from both Arg-35 and Arg-87, the 3′-phosphate interacts with Lys-49 rather than with Lys-84 and Tyr-85. The repositioned thymine ring permits hydrogen bonding to the phenolic hydroxyl of Tyr-115. These new interactions, found in the NMR-docked structure, are supported by reduced affinities for 3′,5′-pdTp by appropriate mutants of staphylococcal nuclease. An inner sphere rather than a second sphere water molecule is optimally positioned to donate a hydrogen bond to the general base, Glu-43, and to attack the coordinated 5′-phosphate with inversion. In accord with the X-ray structure, Arg-87 donates a hydrogen bond to the leaving O5′ atom and probably serves as the general acid catalyst. It may be concluded that the NMR docking procedure can correct structural artifacts created by lattice contacts in crystals, when they occur at or near ligand-binding sites, such as the active sites of enzymes.

ACKNOWLEDGMENTS

Supported by National Institutes of Health Grant DK-28616 to A.S.M. and GM-36358 to E.E.L. D.J.W. is a recipient of a National Institutes of Health National Research Service Award (F32 GM13324).

REFERENCES

1. Tucker, P. W., Hazen, E. E., Jr., Cotton, F. A. Staphylococcal nuclease reviewed: A prototypic study in contemporary enzymology. III. Correlation of the three dimensional structure with the mechanisms of enzymatic action. Mol. Cell. Biochem. 23:67–86, 1979.
2. Anfinsen, C. B., Cuatrecasas, P., Taniuchi, H. Staphylococcal nuclease, chemical properties and catalysis. Enzymes 4:177–204, 1971.
3. Cuatrecasas, P., Fuchs, S., Anfinsen, C. B. Catalytic properties and specificity of the extracellular nuclease of staphylococcus aureus. J. Biol. Chem. 242:1541–1547, 1967.
4. Weber, D. J., Mullen, G. P., Mildvan, A. S. Conformation of an enzyme-bound substrate of staphylococcal nuclease as determined by NMR. Biochemistry 30:7425–7437, 1991.
5. Weber, D. J., Gittis, A. G., Mullen, G. P., Abeygunawardana, C., Lattman, E. E., Mildvan, A. S. NMR docking of a substrate into the x-ray structure of staphylococcal nuclease. Proteins 13:275–287, 1992.
6. Serpersu, E. H., Hibler, D. W., Gerlt, J. A., Mildvan, A. S. Kinetic and magnetic resonance studies of the glutamate-43 to serine mutant of staphylococcal nuclease. Biochemistry 28:1539–1548, 1989.
7. Loll, P. J., Lattman, E. E. The crystal structure of the ternary complex of staphylococcal nuclease, Ca^{2+}, and the inhibitor pdTp refined at 1.65 Å. Proteins 5:183–201, 1989.
8. Fry, D. C., Kuby, S. A., Mildvan, A. S. NMR studies of the MgATP binding site of adenylate kinase and of a 45-residue peptide fragment. Biochemistry 24:4680–4694, 1985.
9. Weber, D. J., Serpersu, E. H., Gittis, A. G., Lattman, E. E., Mildvan, A. S. NMR docking of the inhibitor 3′,5′-pdTp into the x-ray structure of staphylococcal nuclease (SN). Biochemistry 31:2203 (Abs-84), 1992.
10. Chuang, W.-J., Weber, D. J., Gittis, A. G., Mildvan, A. S. Mutational tests of the NMR-docked structure of the staphylococcal nuclease-metal-3′,5′-pdTp complex. Proteins, 17:36–48, 1993.
11. Serpersu, E. H., Shortle, D. R., Mildvan, A. S. Kinetic and magnetic resonance studies of the effects of genetic substitution of a Ca^{2+}-liganding amino acid in staphylococcal nuclease. Biochemistry 25:68–77, 1986.
12. Shortle, D., Meeker, A. K. Residual structure in large fragments of staphylococcal nuclease: Effects of amino acid substitutions. Biochemistry 28:936–944, 1989.
13. Dunn, B. M., DiBello, C., Anfinsen, C. B. The pH dependence of the steady-state kinetic parameters for staphylococcal nuclease catalyzed hydrolysis of deoxythymidine-3′-phosphate-5′-p-nitrophenyl phosphate in H_2O and D_2O. J. Biol. Chem. 248:4769–4774, 1973.
14. Tucker, P. W., Hazen, E. E., Jr., Cotton, F. A. Staphylococcal nuclease reviewed: A prototypic study in contemporary enzymology. I. Isolation, physical and enzymatic properties. Mol. Cell. Biochem. 22:67–77, 1978.
15. Serpersu, E. H., Shortle, D., Mildvan, A. S. Kinetic and magnetic resonance studies of active site mutants of staphylococcal nuclease: Factors contributing to catalysis. Biochemistry 26:1289–1300, 1987.
16. Mildvan, A. S., Gupta, R. K. Nuclear relaxation measurements of the geometry of enzyme-bound substrates and analogs. Methods Enzymol. 49G:322–359, 1978.
17. Mildvan, A. S., Granot, J., Smith, G. M., & Liebman, M. N. The use of paramagnetic probes to determine metal-substrate and intersubstrate distances on enzymes. Adv. Inorg. Biochem. 2:211–236, 1980.
18. Serpersu, E. H., McCracken, J., Peisach, J., Mildvan, A. S. Electron spin echo modulation and nuclear relaxation studies of staphylococcal nuclease and its metal-coordinating mutants. Biochemistry 27:8034–8044, 1988.
19. Tropp, J., Redfield, A. G. Environment of ribothymidine in transfer RNA studied by means of nuclear Overhauser effect. Biochemistry 20:2133–2140, 1981.
20. Rosevear, P. R., Bramson, H. N., O'Brian, C., Kaiser, E. T., Mildvan, A. S. Nuclear Overhauser effect studies of the conformations of tetraaminecobalt(III)ATP free and bound to bovine heart protein kinase. Biochemistry 22:3439–3447, 1983.
21. Rosevear, P. R., Fox, T. L., Mildvan, A. S. Nuclear Overhauser effect studies of the conformations of MgATP bound to the active and secondary sites of muscle pyruvate kinase. Biochemistry 26:3487–3493, 1987.
22. Noggle, J. H., Shirmer, R. E. "The Nuclear Overhauser Effect." New York: Academic Press, 1971.
23. Levitt, M., Warshel, A. Extreme conformational flexibility

of the furanose ring in DNA and RNA. J. Am. Chem. Soc. 100:2607–2613, 1978.
24. Saenger, W. In: "Principles of Nucleic Acid Structure." Cantor, C. R., ed. New York: Springer-Verlag, 1984: 51–104.
25. Ferrin, L. J., Mildvan, A. S. Nuclear overhauser effect studies of the conformations and binding site environments of deoxynucleoside triphosphate substrates bound to DNA polymerase I and its large fragment. Biochemistry 24:6904–6913, 1985.
26. Jeener, J., Meier, B. H., Bachmann, P., Ernst, R. R. Investigation of exchange processes by two-dimensional NMR spectroscopy. J. Chem. Phys. 71:4546–4553, 1979.
27. Kumar, A., Wagner, G., Ernst, R. R., Wüthrich, K. A two-dimensional nuclear Overhauser enhancement (2D-NOE) experiment for the elucidation of complete proton-proton cross relaxation networks in biological macromolecules. Biochem. Biophys. Res. Commun. 96:1156–1163, 1980.
28. Marion, D., Wüthrich, K. Applications of phase sensitive two dimensional correlated spectroscopy (COSY) for measurements of ^1H-^1H spin-spin coupling constants in proteins. Biochem. Biophys. Res. Commun. 113:967–974, 1983.
29. Baleja, J. D., Moult, J., Sykes, B. D. Distance measurement and structure refinment with NOE data. J. Magn. Reson. 87:375–384, 1990.
30. Jones, T. A. A graphics model building and refinement system for macromolecules. J. Appl. Crystallogr. 11:268–272, 1978.
31. Brünger, A. T. XPLOR Manual, Version 2.1, Yale Univ., New Haven, CT, 1990.
32. Nilges, M., Gronenborn, A. M., Brünger, A. T., Clore, G. M. Determination of three dimensional structures of proteins by simulated annealing with interproton distance restraints. Application to crambin, potato carboxypeptidase inhibitor, and barley serine protease inhibitor 2. Protein Eng. 2:27–38, 1988.
33. Brooks, R. R. Bruccoleri, R. E., Olafsen, B. D., States, D. J., Swaminanthan, S., Karplus, M. J. CHARMM, a program for macromolecular energy minimization and dynamics calculations. J. Comput. Chem. 4:187–217, 1983.
34. Stites, W. E., Gittis, A. G., Lattman, E. E., Shortle, D. In a staphylococcal nuclease mutant the side chain of a lysine replacing valine 66 is fully buried in the hydrophobic core. J. Mol. Biol. 221:7–14, 1991.
35. Dao-pin, S., Anderson, D. E., Baase, W. A., Dahlquist, F. W., Matthews, B. W. Structural and thermodynamic consequences of burying a charged residue within the hydrophobic core of T4 lysozyme. Biochemistry 30:11521–11529, 1991.
36. James, T. L. Binding of ADP to creatine kinase. An investigation using intermolecular nuclear Overhauser effect measurements. Biochemistry 15:4724–4730, 1976.
37. Torchia, D. A., Sparks, S. W., Bax, A. Staphylococcal nuclease: Sequential assignments and solution structure. Biochemistry 28:5509–5524, 1989.
38. Wang, J., LeMaster, D. M., Markley, J. L. Two dimensional NMR studies of staphylococcal nuclease. I. Sequence specific assignments of hydrogen-1 signals and solution structure of the nuclease H124L-3′,5′-pdTp-Ca^{2+} ternary complex. Biochemistry 29:88–101, 1990.
39. Poole, L. B., Loveys, D. A., Hale, S. P., Gerlt, J. A., Stanczyk, S. M., Bolton, P. H. Deletion of the Ω loop in the active site of staphylococcal nuclease. 1. Effect on catalysis and stability. Biochemistry 30:3621–3627, 1991.
40. Grissom, C. B., Markley, J. L. Staphylococcal nuclease active site amino acids: pH dependence of tyrosines and arginines by ^{13}C NMR and correlation with kinetic studies. Biochemistry 28:2116–2124, 1989.
41. Cotton, F. A., Hazen, E. E., Jr., Legg, M. J. Staphylococcal nuclease: Proposed mechanism of action based on structure of enzyme-thymidine 3′,5′-bisphosphate-calcium ion complex at 1.5 Å resolution. Proc. Natl. Acad. Sci. U.S.A. 76:2551–2555, 1979.
42. Pourmotabbed, T., Dell'Acqua, M., Gerlt, J. A., Stanczyk, S., Bolton, P. H. Kinetic and conformational effects of lysine substitutions for arginines 35 and 87 in the active site of staphylococcal nuclease. Biochemistry 29:3677–3683, 1990.
43. Sundaralingam, M. The concept of a conformationally 'rigid' nucleotide and its significance in polynucleotide conformational analysis. Jerusalem Symp. Quant. Chem. Biochem. 5:417–456, 1973.
44. Wüthrich, K. "NMR of Proteins and Nucleic Acids." New York: Wiley, 1986.